

TS-DP: Reinforcement Speculative Decoding For Temporal Adaptive Diffusion Policy Acceleration

Ye Li¹ Jiahe Feng^{1,*} Yuan Meng^{1,†} Kangye Ji¹ Chen Tang¹
 Xinwan Wen¹ Shutao Xia¹ Zhi Wang^{1,†} Wenwu Zhu¹

¹Tsinghua University

Abstract

*Diffusion Policy (DP) excels in embodied control but suffers from high inference latency and computational cost due to multiple iterative denoising steps. The temporal complexity of embodied tasks demands a dynamic, adaptable computation mode. Static and lossy acceleration methods (e.g., quantization) fail to handle such dynamic embodied tasks, while speculative decoding offers a lossless, adaptive, yet underexplored alternative for DP. However, it is non-trivial to address the following challenges: (1) How to match the base model’s denoising quality at lower cost under time-varying task difficulty in embodied settings; and (2) How to dynamically interactive adjust computation based on task difficulty in such environments. In this paper, we propose Temporal-aware Reinforcement-based Speculative Diffusion Policy (TS-DP), the first framework that enables speculative decoding for DP with temporal adaptivity. First, to handle dynamic environments where task difficulty varies over time, we distill a Transformer-based drafter to imitate the base model and replace its costly denoising calls. Second, an RL-based scheduler further adapts to the time-varying task difficulty by adjusting speculative parameters to maintain accuracy while improving efficiency. Extensive experiments across diverse embodied environments show that TS-DP achieves up to **4.17**× faster inference with **over 94%** accepted drafts, reaching an inference frequency of **25 Hz** and enabling real-time diffusion-based control without performance degradation.*

1. Introduction

Diffusion Policy (DP) [10] has been widely adopted in Vision-Language-Action (VLA) models [1, 3, 8, 14, 28, 29, 37] thanks to its strong ability to model multi-modal action distributions and generate coherent action trajectories.

*Work done as research intern at Tsinghua University.

†Corresponding authors:
 yuanmeng@tsinghua.edu.cn, wangzhi@sz.tsinghua.edu.cn.

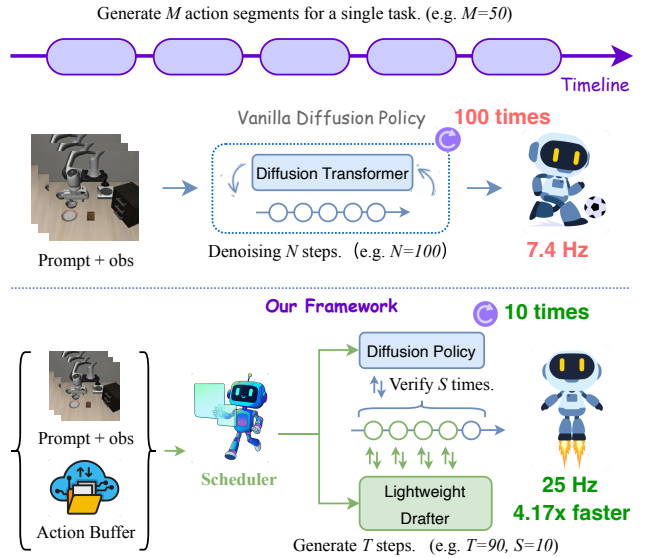


Figure 1. **Vanilla Diffusion Policy vs. Our TS-DP.** For embodied tasks, DP completes a task through multiple interactions with the environment, generating several segments of actions. Each segment typically requires hundreds of model calls for denoising, making the process highly time-consuming. TS-DP introduces a customized speculative decoding framework for temporal-complexity-aware accelerating DP. A lightweight drafter generates multiple denoising results, which are verified in parallel by the DP for lossless acceleration. A scheduler further adjusts key speculative decoding parameters—such as the number of drafts and the acceptance rate—based on the complexity of different task phases, achieving adaptive and efficient acceleration.

However, its large backbone and iterative denoising process impose substantial computational overhead, resulting in low action-generation frequency and limiting its applicability in latency-sensitive real-world settings. Consequently, improving the inference efficiency of DP has therefore emerged as a critical challenge.

Recent research has increasingly focused on accelerating diffusion models (DMs) to enable faster inference. General model compression techniques, including pruning and

quantization [9, 19, 38, 46], reduce computational cost by simplifying the diffusion backbone and have shown effectiveness in static generation tasks. Building on these advances, a growing body of work explores specific acceleration techniques for DP, where cache-based methods [15, 41] reuse intermediate features from previous denoising steps to eliminate redundant computation during action generation. While effective to some extent, these approaches inevitably alter internal feature representations, resulting in *lossy acceleration* and constrained overall speedup. Furthermore, they remain largely static and fail to account for the temporal correlations and evolving task complexity inherent in embodied control.

Meanwhile, speculative decoding has emerged as a lossless and complexity-adaptive acceleration paradigm, where a lightweight drafter proposes multiple candidates that are verified in parallel by a stronger model. This strategy has achieved notable success in LLMs [4, 21, 22, 25], delivering substantial speedups without compromising fidelity, and has also been adapted to DMs by accelerating the denoising process [2, 13]. However, these approaches primarily target compute-bound DMs for image and video generation, where GPU computation dominates and the verification stage offsets most potential savings, resulting in limited acceleration. In contrast, **DP is inherently I/O-bound** as it generates low-dimensional action vectors instead of high-resolution visual data. This property makes speculative decoding particularly well-suited for DP inference. Yet DP differs fundamentally from conventional DMs: it must produce **sequential** action segments while continuously interacting with an evolving environment, where task difficulty and dynamics change over time, making temporal adaptivity essential for stable and efficient acceleration. As a result, temporal adaptivity becomes crucial for maintaining both stability and efficiency. This motivates a temporal-complexity-aware speculative decoding framework that preserving behavioral consistency and robust control performance.

Therefore, we propose TS-DP, the first temporal-complexity-aware speculative decoding framework designed to accelerate DP, as illustrated in Fig. 1. This presents two key challenges: (1) how to match the base model’s denoising quality at lower cost under time-varying task difficulty, and (2) how to dynamically adjust computation based on task difficulty to ensure stable and efficient control.

For the first challenge, prior studies [2, 13] leverage either the differences between consecutive time steps as drafts or the exchangeability of trajectories to enable self-speculation and parallel verification. However, embodied tasks are highly diverse, and their multi-segment action sequences often exhibit significant distributional differences, making these approaches difficult to generalize and largely limited to image generation. To address this, we adopt a single Transformer block as the drafter and train it via knowledge distillation, where DP serves as the teacher and the drafter

is optimized to minimize both its deviation from the ground truth and its discrepancy from the teacher’s outputs. The drafter shares the same input–output interface as DP, performs multiple denoising steps in its place, and has its results verified in parallel by DP. During each speculative decoding round, accepted denoising steps are retained, while the first rejected one is corrected via Reflection-Maximal Coupling to match DP’s probability distribution. This process repeats iteratively until the denoising is complete.

For the second challenge, the temporal characteristics of embodied tasks cause task difficulty to vary dynamically over time. As shown in Fig. 4, empirical analysis reveals an inverse relationship between end-effector velocity and the number of accepted drafts—faster, coarse-grained motions lead to fewer accepted drafts, while slower, fine-grained actions yield more. This indicates that using fixed parameters for speculative decoding is suboptimal. Existing approaches, such as SP-VLA [23], distinguish task difficulty only by velocity, which limits their generalization across diverse behaviors. To address this, we introduce a Reinforcement Learning (RL)-based scheduler that dynamically adjusts speculative decoding parameters according to task phase, enabling adaptive and efficient acceleration. Extensive experiments demonstrate that TS-DP achieves approximately 94% draft acceptance, resulting in a $4.17 \times$ reduction in Number of Function Evaluations (NFE) and an inference frequency of 25 Hz, while maintaining lossless performance. The main contributions of TS-DP are as follows:

- (1) We propose TS-DP, a temporal-complexity-aware speculative decoding framework for DP, enabling frequency-adaptive and lossless acceleration. To the best of our knowledge, this is the first work that brings speculative decoding to DP with temporal adaptivity.
- (2) We propose a speculative decoding framework tailored for DP. To match the base model’s denoising quality at lower cost under time-varying task difficulty, we distill a Transformer-based drafter to imitate the base model and replace its costly multi-step denoising calls, while DP verifies its outputs in parallel.
- (3) We propose a temporal-complexity-aware speculative decoding scheduler. To dynamically adjust computation based on task difficulty, we train a PPO-based scheduler that formulates DP execution as a Markov process and adaptively tunes speculative parameters over time.

2. Related Work

2.1. Diffusion Policy Acceleration

DP has become a leading framework for visuomotor policy learning, leveraging the generative capability of DMs to produce continuous and multimodal robotic actions conditioned on visual observations and language instructions [10, 31]. Despite their strong performance, DP suffer from high infer-

ence latency caused by iterative denoising, which limits their applicability in real-time, high-frequency robotic control.

To tackle this challenge, extensive research has focused on accelerating diffusion-based generative models and their extensions to embodied policies [11, 20, 23, 24, 30, 32, 44]. A variety of techniques are applied to accelerate diffusion models in the field of image and video generation, such as quantization [5, 9, 12, 19, 35, 42, 45], feature cache [26, 27, 47, 48, 50, 51], and one-step sampler [33, 36, 39, 43, 49]. In contrast, EfficientVLA [40] and BAC [15] are specifically designed for DP acceleration, where the latter introduces block-wise adaptive caching to selectively refresh upstream features and mitigate error propagation. However, most existing methods modify intermediate representations during inference, resulting in lossy acceleration, and few explicitly account for the temporal redundancy inherent in DP.

2.2. Speculative Decoding

Speculative decoding has recently emerged as a principled paradigm for accelerating autoregressive generation. Originally developed for LLMs [6, 7, 16–18], it employs a lightweight *drafter* to propose multiple future tokens that are verified in parallel by a stronger *target* model within a single forward pass, achieving provable lossless acceleration. Representative approaches such as the Medusa and Eagle series [4, 21, 22, 25] further enhance efficiency through multi-head drafting and hierarchical verification mechanisms.

Beyond LLMs, several studies have extended speculative decoding to continuous generative processes. [2] introduced the frozen target draft model, which accelerates diffusion denoising by using stepwise differences as drafts and applies reflection-maximal coupling to preserve the original sampling distribution. Building on this, [13] proposed autospeculative decoding, eliminating the need for a separate drafter by exploiting trajectory exchangeability for self-speculation and parallel verification. While these methods achieve lossless acceleration in DDPMs and LDMs, they are primarily designed for compute-bound diffusion models in image and video generation, and the verification overhead largely cancels out the benefit—resulting in the counterintuitive phenomenon that even using 8 GPUs for verification yields only about a $1.8\times$ speedup.

In contrast, DP is inherently I/O-bound and therefore better suited for speculative decoding. The drafter operates at a much lower computational cost than the base policy, allowing parallel verification to be substantially more efficient than in compute-bound diffusion models. However, unlike standard DMs, DP must generate sequential action segments through interactions with the environment, where early prediction errors can accumulate and degrade overall task performance. To address these challenges, we introduce **TS-DP**, a temporal-complexity-aware speculative decoding framework that enables adaptive, lossless acceleration for

embodied tasks.

3. Method

3.1. Preliminaries

Speculative decoding. Speculative decoding leverages a lightweight draft model p to generate a short trajectory of length L in a single forward pass, while the large-scale target model q verifies the generated drafts in parallel. This approach reduces the number of target model invocations, thereby improving inference efficiency. The joint distribution of the drafted latents is formulated as:

$$\tilde{\mathbf{x}}_{t+1:t+L} \sim p(\tilde{\mathbf{x}}_{t+1:t+L} \mid \mathbf{x}_t) = \prod_{j=1}^L p(\tilde{\mathbf{x}}_{t+j} \mid \tilde{\mathbf{x}}_{t+1:t+j-1}, \mathbf{x}_t), \quad (1)$$

where \mathbf{x}_t denotes the current diffusion latent at timestep t , and $\tilde{\mathbf{x}}_{t+j}$ denotes the j -th drafted latent. Each drafted latent is accepted according to the standard likelihood-ratio test:

$$\alpha_j(\tilde{\mathbf{x}}_{t+j}) = \min\left(1, \frac{q(\tilde{\mathbf{x}}_{t+j} \mid \tilde{\mathbf{x}}_{t+1:t+j-1}, \mathbf{x}_t)}{p(\tilde{\mathbf{x}}_{t+j} \mid \tilde{\mathbf{x}}_{t+1:t+j-1}, \mathbf{x}_t)}\right). \quad (2)$$

The first rejection index is defined as:

$$j^* = \min\{j \in \{1, \dots, L\} : U_j > \alpha_j(\tilde{\mathbf{x}}_{t+j})\}, \quad (3)$$

where $U_j \sim \text{Unif}(0, 1)$ are independent uniform random variables. All drafted latents after j^* are discarded, and a corrective coupling is applied at step $t + j^* - 1$ to obtain a latent consistent with the target distribution.

The window length L and the closeness of p to q jointly control the trade-off between parallelism and the probability of encountering a rejection within the window.

Reflection-maximal coupling. For continuous, approximately Gaussian one-step conditionals, we apply *reflection-maximal coupling* to correct the first rejected draft sample through a single deterministic mapping. Let

$$r(\mathbf{x}) = \mathcal{N}(\mathbf{x}; \mathbf{m}_r, \Sigma), \quad s(\mathbf{x}) = \mathcal{N}(\mathbf{x}; \mathbf{m}_s, \Sigma), \quad (4)$$

where $r(\mathbf{x})$ and $s(\mathbf{x})$ denote the draft and target Gaussian densities with means \mathbf{m}_r and \mathbf{m}_s and shared covariance Σ . Draw $\tilde{\mathbf{x}} \sim r$ and perform the acceptance test:

$$A = \mathbf{1}\left(U \leq \min\left(1, \frac{s(\tilde{\mathbf{x}})}{r(\tilde{\mathbf{x}})}\right)\right), \quad U \sim \text{Unif}(0, 1). \quad (5)$$

If $A = 1$, accept $\mathbf{x} = \tilde{\mathbf{x}}$. If $A = 0$, obtain a corrected sample by reflecting $\tilde{\mathbf{x}}$ across the hyperplane orthogonal to $\Delta := \mathbf{m}_r - \mathbf{m}_s$. In the isotropic case $\Sigma = \sigma^2 \mathbf{I}$, the reflection takes the form:

$$\mathbf{x} = \mathbf{m}_s + (\mathbf{I} - 2\mathbf{e}\mathbf{e}^\top)(\tilde{\mathbf{x}} - \mathbf{m}_r), \quad \mathbf{e} := \frac{\Delta}{\|\Delta\|_2}. \quad (6)$$

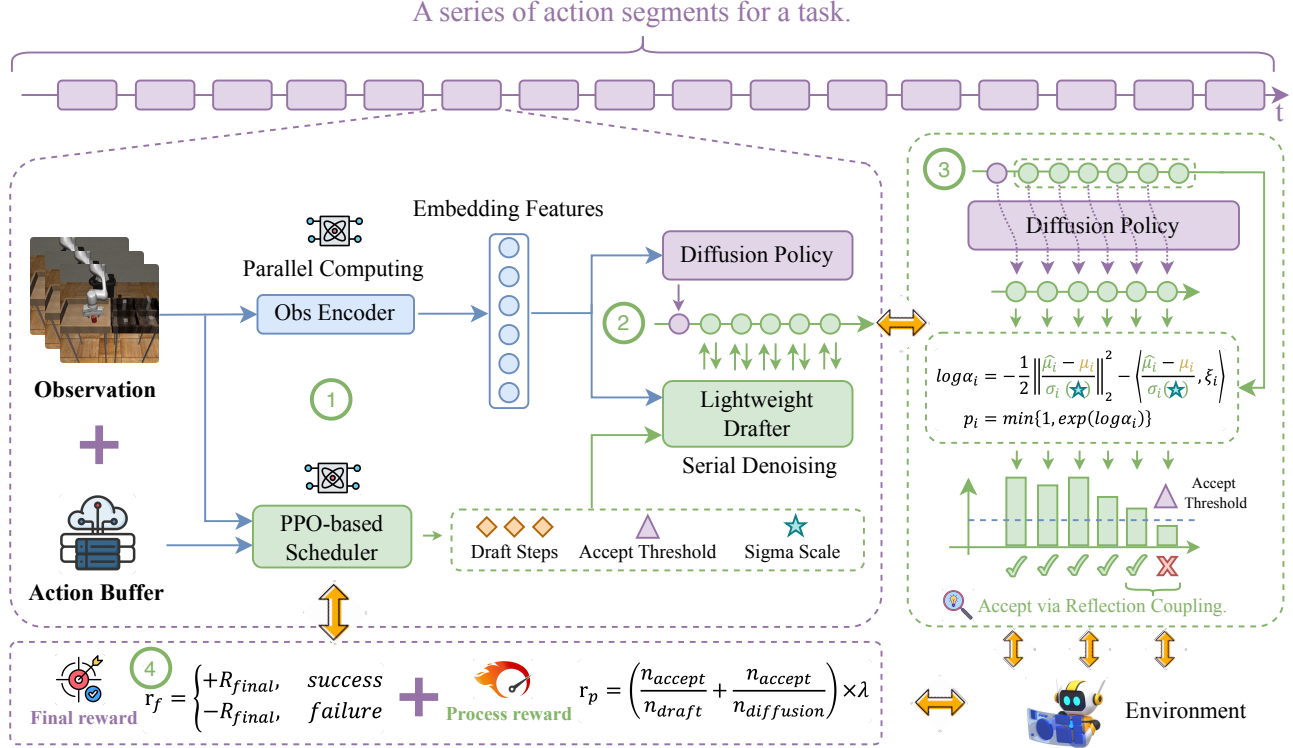


Figure 2. **The framework of TS-DP.** TS-DP is the first temporal-aware speculative decoding framework designed to accelerate Diffusion Policy. ① **Decision stage:** A PPO-based scheduler evaluates time-varying task difficulty using past observations and actions, and produces adaptive speculative parameters. It operates in parallel with the observation encoder, adding no extra inference latency. ② **Denoising stage:** Guided by the scheduler, a lightweight drafter executes multiple denoising steps sequentially, effectively replacing expensive DP calls and reducing computational load. ③ **Verification stage:** DP verifies all drafted steps in parallel, accepting those that pass validation and correcting the first rejected draft via reflection-maximal coupling to match the target distribution. ④ **Reward generation:** Based on task progress, the framework provides process rewards that encourage the scheduler to produce more valid drafts, and a final success-driven reward upon task completion, jointly guiding the scheduler toward efficient and successful task execution.

Equations 4–6 depend only on the means \mathbf{m}_r , \mathbf{m}_s , the shared covariance Σ , and a single draw $\tilde{\mathbf{x}} \sim r$. The mapping in Eq. (6) generates a sample whose marginal distribution follows s , while minimizing the discrepancy between the rejected draft and its corrected counterpart.

3.2. Speculative Drafting and Verification Framework

Draft Model Training. The draft model is a lightweight approximator of the target model, designed for fast speculative rollouts while maintaining behavioral alignment. Since a lightweight architecture is sufficient for approximate denoising, we employ a single-layer Transformer block as the draft model, which shares the same encoder and DDPM or DDIM scheduler with the target model M_ϕ . This design effectively reduces the number of target model invocations and improves inference efficiency.

Specifically, we train the draft model \hat{M}_θ via knowledge distillation with two objectives. (1) The first component is a prediction-level distillation loss that aligns the draft model

output $\hat{\mathbf{m}}_t^\theta$ with the target model output \mathbf{m}_t^ϕ :

$$\mathcal{L}_{\text{pred}}(\theta) = \mathbb{E}_{t, \mathbf{x}_0, \epsilon} \left\| \hat{\mathbf{m}}_t^\theta - \mathbf{m}_t^\phi \right\|_2^2, \quad (7)$$

where t is the diffusion timestep, \mathbf{x}_0 is the clean action, and ϵ is the Gaussian noise used to construct the noisy latent. (2) The second component is a scheduler-aware normalized loss that aligns the draft model with the data-consistent denoising behavior of the target model:

$$\mathcal{L}_{\text{norm}}(\theta) = \mathbb{E}_{t, \mathbf{x}_0, \epsilon} \left\| \frac{\hat{\mu}_t^\theta - \mu_t^\phi}{\sigma_t} \right\|_2^2, \quad (8)$$

where μ_t^ϕ and $\hat{\mu}_t^\theta$ are the data-aligned DDPM means computed from the target and draft predictions, and σ_t is the DDPM standard deviation at timestep t .

The full objective combines both terms:

$$\mathcal{L}(\theta) = \lambda_1 \mathcal{L}_{\text{pred}}(\theta) + \lambda_2 \mathcal{L}_{\text{norm}}(\theta), \quad (9)$$

Table 1. **Benchmark on Proficient Human (PH) demonstration data.** Accuracy, NFE, and acceleration performance are reported. TS-DP achieves a $4.17\times$ acceleration on such tasks, while also improving accuracy by 9%.

Method	Success Rate (% , ↑)						AVG (%, ↑)	NFE (%, ↓)	Speed ×
	Lift	Can	Square	Transport	Tool	Push-T			
Diffusion Policy [10]	100 / 100	95 / 97	82 / 88	78 / 81	43 / 53	59 / 64	76 / 80	100 / 100	–
Frozen Target Draft [2]	90 / 92	82 / 84	70 / 70	50 / 64	26 / 34	16 / 17	56 / 60	33 / 32	3.03 / 3.13
SpeCa [27]	100 / 100	92 / 96	88 / 88	68 / 72	38 / 40	67 / 69	76 / 78	34 / 35	2.94 / 2.86
BAC [15]	100 / 100	94 / 97	82 / 89	77 / 82	49 / 55	59 / 62	77 / 81	– / –	3.40 / 3.40
TS-DP	100 / 100	95 / 95	86 / 88	87 / 84	61 / 52	79 / 63	85 / 80	24 / 24	4.17 / 4.17

with $\lambda_1, \lambda_2 > 0$. The target model parameters ϕ are kept frozen throughout training, while only the draft parameters θ are updated.

Draft Generation Procedure. During the inference phase, speculative drafts are generated through a short and efficient forward rollout using the lightweight draft model, conditioned on the current denoised estimate produced by the target model. Let M denote the target model and \mathcal{S} the DDPM scheduler. At each time step t , the target model predicts the noise estimate $\mathbf{m}_t = M(\mathbf{x}_t; t)$, and the scheduler \mathcal{S} produces the immediate one-step denoised candidate $\mathbf{x}_{t-1}^{(0)} = \mathcal{S}(\mathbf{m}_t, t, \mathbf{x}_t)$.

Starting from $\mathbf{x}_{t-1}^{(0)}$, a lightweight draft model \hat{M} performs an autoregressive-style multi-step rollout for up to K steps. For each draft step $k = 1, \dots, K$, we compute the draft prediction at time $t - k$ and apply the same DDPM scheduler to obtain the next draft sample:

$$\begin{aligned} \hat{\mathbf{m}}_{t-k} &= \hat{M}\left(\mathbf{x}_{t-k+1}^{(\text{draft})}; t - k\right), \\ \mathbf{x}_{t-k}^{(\text{draft})} &= \mathcal{S}\left(\hat{\mathbf{m}}_{t-k}, t - k, \mathbf{x}_{t-k+1}^{(\text{draft})}\right). \end{aligned} \quad (3)$$

This rollout continues until either the maximum draft horizon K is reached or the diffusion process arrives at $t = 0$. Throughout the rollout, we retain all draft-model outputs and scheduler intermediates—including predicted means, variances, and the random noise realizations used during sampling—for use in the subsequent verification and acceptance stage.

As shown in Fig. 3a, the acceptance probability displays clear phase-dependent trends: it is low during both the early high-noise and late low-noise stages, while remaining high and stable throughout the intermediate denoising phase. To balance acceleration and sample fidelity along the denoising trajectory, we treat the draft horizon K as an adaptive hyperparameter that depends on the current timestep. A smaller K is used in the early high-noise and late low-noise stages, while a larger K is applied in the intermediate phase where the signal-to-noise ratio is moderate and predictions are more reliable. To enable fine-grained adjustment across

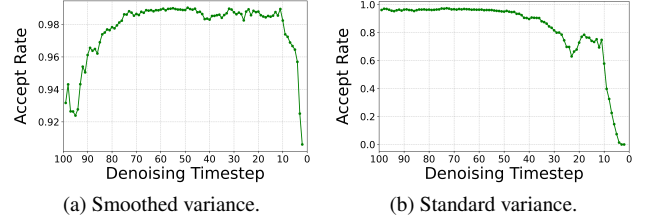


Figure 3. **Impact of Drafter Parameters on Draft Acceptance Rate.** Evolution of Metropolis–Hastings acceptance probability throughout the 100-step denoising process.

different task stages, TS-DP dynamically tunes this parameter through the scheduler, maintaining high draft acceptance and maximizing speedup without compromising perceptual quality.

Verification of Speculative Drafts. Given the one-step candidate $\mathbf{x}_{t-1}^{(0)}$ from the target model and a sequence of K draft proposals $\{\mathbf{x}_{t-1}^{(1)}, \mathbf{x}_{t-2}^{(2)}, \dots, \mathbf{x}_{t-K}^{(K)}\}$ generated by the draft model, we form the candidate set \mathcal{C} . Verification is performed by evaluating the frozen target model M_ϕ on all elements of \mathcal{C} in a single batched forward pass. Using the DDPM scheduler, we obtain for each candidate the conditional mean μ_i and the effective standard deviation σ_i . As shown in Fig. 3b, the standard deviation is crucial for draft acceptance. Without proper adjustment, the acceptance probability collapses to nearly 0 in the later denoising stages due to numerical overconfidence, severely degrading speculative efficiency. Therefore, we treat σ_i as a hyperparameter and allow the scheduler to dynamically adjust it according to task complexity. This adaptive adjustment maintains stable acceptance probabilities throughout the denoising trajectory, enabling consistent speculative acceleration.

Under the Gaussian conditional distribution induced by the DDPM scheduler, the log acceptance ratio for the i -th draft sample $\mathbf{x} = \hat{\mu}_i + \sigma_i \xi_i$ (with $\xi_i \sim \mathcal{N}(\mathbf{0}, \mathbf{I})$) in a Metropolis–Hastings test is:

$$\log \alpha_i = -\frac{1}{2} \left\| \frac{\hat{\mu}_i - \mu_i}{\sigma_i} \right\|_2^2 - \left\langle \frac{\hat{\mu}_i - \mu_i}{\sigma_i}, \xi_i \right\rangle. \quad (10)$$

Table 2. **Benchmark on Mixed Human (MH) demonstration data.** Accuracy, NFE, and acceleration performance are reported. TS-DP achieves lossless accuracy on this task while delivering a $3.84\times$ acceleration.

Method	Success Rate (% , \uparrow)				AVG (%, \uparrow)	NFE (%, \downarrow)	Speed \times
	Lift	Can	Square	Transport			
Diffusion Policy [10]	99 / 100	92 / 97	76 / 79	35 / 46	76 / 81	100 / 100	–
Frozen Target Draft [2]	66 / 62	60 / 54	50 / 62	20 / 42	49 / 55	34 / 33	2.94 / 3.03
SpeCa [27]	96 / 100	86 / 90	76 / 68	34 / 40	73 / 75	35 / 37	2.86 / 2.70
BAC [15]	99 / 98	95 / 97	77 / 79	30 / 46	75 / 80	– / –	3.41 / 3.41
TS-DP	99 / 99	92 / 97	74 / 78	34 / 62	75 / 84	26 / 26	3.84 / 3.84

Table 3. **Benchmark on multi-stage task (Kitchen & BP).** In the Kitchen task, p_x denotes the frequency of interacting with x or more objects (e.g., microwave, burners, oven switch, kettle). In the BP task, p_x represents the success rate under progressively harder control phases. TS-DP achieves lossless accuracy on this task while delivering a $3.7\times$ acceleration.

Method	Success Rate (% , \uparrow)						AVG (%, \uparrow)	NFE (%, \downarrow)	Speed \times
	BP _{p1}	BP _{p2}	Kit _{p1}	Kit _{p2}	Kit _{p3}	Kit _{p4}			
Diffusion Policy [10]	98 / 98	98 / 96	100 / 100	100 / 100	100 / 100	100 / 100	99 / 99	100 / 100	–
Frozen Target Draft [2]	85 / 86	1 / 2	100 / 100	100 / 100	100 / 100	100 / 100	81 / 81	33 / 33	3.03 / 3.03
SpeCa [27]	97 / 97	85 / 85	100 / 100	100 / 100	100 / 100	100 / 100	97 / 97	37 / 37	2.70 / 2.70
BAC [15]	100 / 99	97 / 95	100 / 99	100 / 99	100 / 99	94 / 97	99 / 98	– / –	3.60 / 3.60
TS-DP	99 / 100	97 / 97	100 / 100	100 / 100	100 / 100	100 / 100	99 / 99	27 / 27	3.70 / 3.70

The corresponding acceptance probability is computed as:

$$p_i = \min\{1, \exp(\log \alpha_i)\}. \quad (11)$$

We accept the draft if $p_i \geq \lambda$, where $\lambda \in (0, 1]$ is a tunable acceptance threshold; otherwise, it is rejected. As shown in Fig. 4, the number of accepted drafts is generally inversely related to the end-effector velocity—more drafts are accepted during slower motions, while fewer are accepted at higher speeds. This observation aligns with the typical behavior of embodied agents, which perform coarse, high-speed actions such as locomotion and fine, low-speed actions such as grasping [23]. However, the non-strict correlation between velocity and acceptance rate indicates that task complexity also plays a critical role. Hence, using fixed speculative decoding parameters is suboptimal for embodied control. To address this, we treat λ as an adaptive hyperparameter that the scheduler dynamically adjusts according to task complexity and velocity. This design enables adaptive speculative decoding and achieves efficient, stable acceleration across diverse task phases.

Finally, we scan the candidates in chronological order, committing all consecutive drafts that are accepted until the first rejection occurs. For the first rejected draft, we apply the reflection coupling algorithm to construct a corrected sample that preserves the original stochasticity while better aligning with the target distribution.

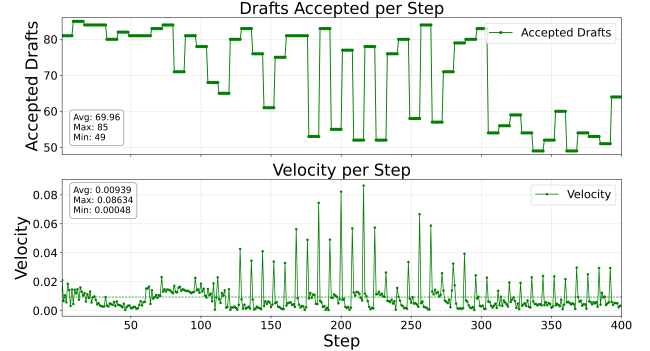


Figure 4. **Effect of End-Effector Velocity on the Number of Accepted Drafts.** Variation of Accepted Drafts and Velocity During the Can-ph Task: (Top) Accepted Drafts per Step; (Bottom) Velocity per Step.

3.3. Temporal-Complexity-Aware Speculative Decoding Scheduler

Markov Modeling for Speculative Decoding. To enable dynamic decision-making of speculative decoding parameters at each time step and train the RL model, we first formulate the speculative decoding process as a Markov chain with a fixed number of steps. Specifically, we integrate the DP, drafter, and embodied simulation environment into a unified interactive system. (1) **The observation space** comprises

three components: the object states returned by the embodied environment (either images or state vectors), the embodied actions generated by DP at each time step, and the current task progress. (2) **The action space** includes the sigma scale, acceptance threshold, and draft step configurations for the three distinct denoising stages.

We adopt a RL-based scheduler implemented with Proximal Policy Optimization (PPO) [34], as it provides stable policy updates and efficient adaptation to continuous task variations. In terms of network design, we separately encode the observation, action, and process streams to prevent interference caused by their differing dimensionalities. The extracted features are then aggregated using an MLP. When the observation is an image, a CNN is employed for feature extraction; otherwise, an MLP is used.

Reward function. The reward function aims to balance accuracy and efficiency, and is therefore divided into two components: the final reward and the intermediate reward. The final reward serves as the primary objective of the scheduler, aiming to ensure task accuracy. It is categorized into two types: discrete outcomes and continuous outcomes:

$$r_{\text{final},\text{dis}} = \begin{cases} +R_{\text{final}}, & \text{success,} \\ -R_{\text{final}}, & \text{failure.} \end{cases} \quad (12)$$

$$r_{\text{final},\text{con}} = 2 \times R_{\text{final}} \times r_{\text{max}} - R_{\text{final}}, \quad (13)$$

where R_{final} is a hyperparameter. This distinction enables us to differentiate between completion-based tasks and binary success–failure tasks.

To transform the sparse rewards into dense ones, we design the intermediate reward as an efficiency metric:

$$r_{\text{process}}^{(i)} = \left(\frac{n_{\text{accept}}}{n_{\text{draft}}} + \frac{n_{\text{accept}}}{n_{\text{diffusion}}} \right) \times \lambda, \quad (14)$$

where n_{accept} , n_{draft} and $n_{\text{diffusion}}$ denote the number of accepted drafts, the total number of drafts, and the number of diffusion steps per denoising cycle, respectively. λ is a scaling factor that constrains the accumulated process reward to one-fourth of the final reward, encouraging the scheduler to pursue efficiency while maintaining accuracy:

$$\lambda = \frac{R_{\text{final}}/4}{N_{\text{expected}}}, \quad N_{\text{expected}} = \left\lceil \frac{T_{\text{max}}}{\Delta t} \right\rceil, \quad (15)$$

where T_{max} is the max task steps, Δt denotes the parameter update frequency.

Furthermore, to reduce computational overhead, the scheduler is executed in parallel with the encoder. As the encoder is significantly larger in scale, the scheduler incurs no additional time cost.

4. Experiments

In this section, we present comprehensive experimental results to demonstrate the superior performance of TS-DP.

Table 4. **Performance Comparison With and Without Scheduler.** TS-DP achieves a $3.8\times$ acceleration while maintaining lossless accuracy.

Method	Success Rate (% ,↑)				AVG (% ,↑)	Speed ×
	Lift	Can	Square	Transport		
K=10	100	94	76	66	84	2.45
K=25	88	88	62	60	75	3.47
K=40	74	90	64	60	72	3.92
TS-DP	100	96	84	66	87	3.80

Table 5. **Frequency and Latency Evaluation of TS-DP.** Compared with DP, TS-DP increases the control frequency by $3.6\times$, reaching 25 Hz.

Method	Frequency (Hz, ↑) / Latency (s, ↓)				AVG
	Lift	Can	Square	Transport	
DP	7.69 / 0.13	7.14 / 0.14	7.14 / 0.14	7.69 / 0.13	7.42 / 0.14
TS-DP	25.00 / 0.04	25.00 / 0.04	25.00 / 0.04	25.00 / 0.04	25.00 / 0.04

Following the original settings in DP [10], we adopt DP as our base model for evaluation. We evaluate TS-DP across 4 different robot manipulation benchmarks with fixed seeds: Robomimic, Push-T, Multimodal Block Pushing, and Kitchen.

Baselines. We compare TS-DP against the unaccelerated DP [10] baseline and 3 representative acceleration methods: 2 speculative decoding techniques, namely Frozen Target Draft [2] and SpeCa [27], along with one caching-based approach BAC [15], are all built upon the identical underlying model architecture.

Evaluation Metrics. For most tasks, the primary precision metric is Success Rate, while Push-T and Block Push use target area coverage instead. Efficiency is measured in terms of Number of Function Evaluations (NFE) and inference speedup during action generation. Since the DP consists of 8 Transformer blocks while the drafter contains only one, each drafter evaluation is counted as 1/8 NFE and each target model evaluation as 1 NFE. All experiments are run on NVIDIA A100 GPUs (40GB).

4.1. Main Results

Tables 1 and 2 present the acceleration performance of TS-DP across different benchmarks. On the PH dataset, TS-DP achieves a $4.17\times$ inference speedup with 76% reduction in NFE while achieving higher success rates of 85 / 80 compared to the baseline DP’s 76 / 80. On the more challenging MH dataset, our method achieves a $3.84\times$ speedup with 76% NFE reduction while achieving success rates of 75 / 84 compared to the baseline’s 76 / 81. For complex multi-stage tasks, Table 3 shows consistent acceleration benefits. On the Kitchen benchmark and Block Pushing tasks, TS-DP achieves a $3.70\times$ speedup with 73% NFE reduction while

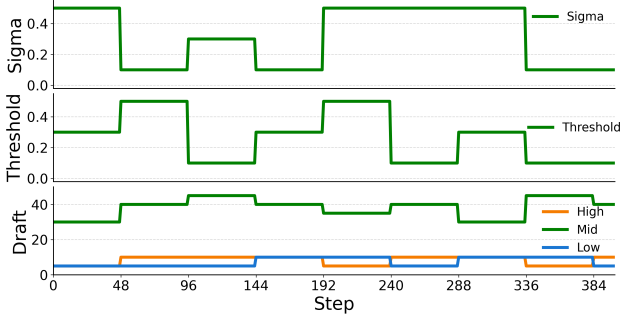


Figure 5. Temporal Variation of Speculative Decoding Parameters. Over time, TS-DP adaptively tunes the parameters of speculative decoding, achieving optimal acceleration across different levels of task difficulty.

maintaining high performance, with an average success rate of 99 / 99 across subtasks.

Compared with baseline methods, TS-DP consistently demonstrates superior acceleration ratios with better task performance across all benchmarks. These results confirm that TS-DP effectively exploits redundancies in the diffusion process, substantially improving inference efficiency without sacrificing policy performance.

4.2. Ablation Study

Effectiveness of Adaptive Scheduling. To validate the efficiency of our scheduler, we conduct an ablation study by fixing all scheduling hyperparameters except the draft step count K during the denoising process. As shown in Table 4, static configurations of K (10, 25, and 40) demonstrate an inherent trade-off between acceleration and accuracy: the conservative $K = 10$ achieves the highest average success rate of 84% but only $2.45 \times$ speedup, while the aggressive $K = 40$ yields the highest acceleration of $3.92 \times$ but suffers significant performance degradation to 72% average success rate. Critically, our adaptive scheduler dynamically adjusts K based on temporal complexity, achieving both superior task performance at 87% average success rate and high acceleration at $3.80 \times$ speedup. This demonstrates that fixed speculative decoding hyperparameters are fundamentally unable to maintain both high performance and acceleration across temporally varying embodied tasks, while our RL-based scheduler effectively optimizes this trade-off by dynamically adapting multiple parameters to the current denoising phase and task requirements.

Latency Analysis. We further evaluate the practical inference latency of TS-DP, measuring the wall-clock time required for single action prediction across different robotic manipulation tasks. As reported in Table 5, the baseline DP requires 0.14s per action prediction, limiting its applicability in high-frequency control scenarios. Our TS-DP framework reduces this latency to 0.04s, achieving a $3.17 \times$ speedup

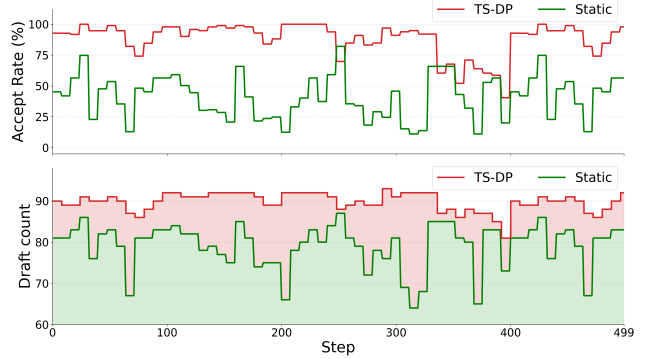


Figure 6. Effect of TS-DP on Acceptance Rate and Draft Count. (Top) Acceptance Rate; (Bottom) Draft Count. With the integration of TS-DP, more drafts are accepted while maintaining task accuracy.

while maintaining identical or better task performance. Notably, TS-DP achieves an average prediction frequency of 25.00 Hz compared to DP’s 7.42 Hz, well exceeding the minimum requirement for real-time robotic control. This latency profile enables TS-DP to meet the timing requirements of real-time robotic control without compromising decision quality, making it suitable for practical deployment on edge devices with limited computational resources.

Visualizations. Fig. 5 demonstrates how controller dynamically adjusts speculative decoding hyperparameters throughout task execution, adapting to varying temporal complexity. As shown in Fig. 6, this adaptive approach yields significantly higher draft acceptance rates and more efficient parallel computation compared to static methods. The red curves (with scheduling) consistently maintain higher acceptance while generating more drafts, demonstrating optimal trade-off between acceleration and accuracy. This confirms that fixed-parameter speculative decoding is limited in embodied tasks with time-varying complexity, while our framework achieves superior end-to-end performance through intelligent hyperparameter adaptation.

5. Conclusion

In this work, we present TS-DP, a temporal-aware speculative decoding framework that accelerates Diffusion Policy by combining efficient draft generation with adaptive scheduling. A distilled Transformer-based drafter replaces expensive base-model denoising calls across multiple steps, while an RL-based scheduler dynamically adjusts speculative parameters based on task difficulty to maintain accuracy and maximize efficiency. Extensive experiments across 4 robotic manipulation benchmarks demonstrate up to $4.17 \times$ faster inference, 76% NFE reduction, and real-time operation at 25 Hz, all achieved without performance degradation.

References

[1] Kevin Black, Noah Brown, Danny Driess, Adnan Esmail, Michael Equi, Chelsea Finn, Niccolò Fusai, Lachy Groom, Karol Hausman, Brian Ichter, et al. π_0 : A vision-language-action flow model for general robot control. *arXiv preprint arXiv:2410.24164*, 2024. 1

[2] Valentin De Bortoli, Alexandre Galashov, Arthur Gretton, and Arnaud Doucet. Accelerated diffusion models via speculative sampling. *ArXiv*, abs/2501.05370, 2025. 2, 3, 5, 6, 7

[3] Anthony Brohan, Noah Brown, Justice Carbajal, Yevgen Chebotar, Xi Chen, Krzysztof Choromanski, Tianli Ding, Danny Driess, Avinava Dubey, Chelsea Finn, et al. Rt-2: Vision-language-action models transfer web knowledge to robotic control. *arXiv preprint arXiv:2307.15818*, 2023. 1

[4] Tianle Cai, Yuhong Li, Zhengyang Geng, Hongwu Peng, and Tri Dao. Medusa: Simple framework for accelerating llm generation with multiple decoding heads, 2023. 2, 3

[5] Hanwen Chang, Haihao Shen, Yiyang Cai, Xinyu Ye, Zhenzhong Xu, Wenhua Cheng, Kaokao Lv, Weiwei Zhang, Yintong Lu, and Heng Guo. Effective quantization for diffusion models on cpus. *arXiv preprint arXiv:2311.16133*, 2023. 3

[6] Charlie Chen, Sebastian Borgeaud, Geoffrey Irving, Jean-Baptiste Lespiau, Laurent Sifre, and John Jumper. Accelerating large language model decoding with speculative sampling. *arXiv preprint arXiv:2302.01318*, 2023. 3

[7] Charlie Chen, Sebastian Borgeaud, Geoffrey Irving, Jean-Baptiste Lespiau, L. Sifre, and John M. Jumper. Accelerating large language model decoding with speculative sampling. *ArXiv*, abs/2302.01318, 2023. 3

[8] Hao Chen, Jiaming Liu, Chenyang Gu, Zhuoyang Liu, Renrui Zhang, Xiaoqi Li, Xiao He, Yandong Guo, Chi-Wing Fu, Shanghang Zhang, et al. Fast-in-slow: A dual-system foundation model unifying fast manipulation within slow reasoning. *arXiv preprint arXiv:2506.01953*, 2025. 1

[9] Lei Chen, Yuan Meng, Chen Tang, Xinzhu Ma, Jingyan Jiang, Xin Wang, Zhi Wang, and Wenwu Zhu. Q-dit: Accurate post-training quantization for diffusion transformers. In *Proceedings of the Computer Vision and Pattern Recognition Conference*, pages 28306–28315, 2025. 2, 3

[10] Cheng Chi, Siyuan Feng, Yilun Du, Zhenjia Xu, Eric Cousineau, Benjamin Burchfiel, and Shuran Song. Diffusion policy: Visuomotor policy learning via action diffusion. *Int. J. Robotics Res.*, 44:1684–1704, 2023. 1, 2, 5, 6, 7

[11] Weifan Guan, Qinghao Hu, Aosheng Li, and Jian Cheng. Efficient vision-language-action models for embodied manipulation: A systematic survey. *arXiv preprint arXiv:2510.17111*, 2025. 3

[12] Yefei He, Luping Liu, Jing Liu, Weijia Wu, Hong Zhou, and Bohan Zhuang. Ptqd: Accurate post-training quantization for diffusion models. *arXiv preprint arXiv:2305.10657*, 2023. 3

[13] Hengyuan Hu, Aniket Das, Dorsa Sadigh, and Nima Anari. Diffusion models are secretly exchangeable: Parallelizing ddpm via autospeculation. *ArXiv*, abs/2505.03983, 2025. 2, 3

[14] Physical Intelligence, Kevin Black, Noah Brown, James Darpinian, Karan Dhabalia, Danny Driess, Adnan Esmail, Michael Equi, Chelsea Finn, Niccolò Fusai, et al. $\pi_{0.5}$: A vision-language-action model with open-world generalization. *arXiv preprint arXiv:2504.16054*, 2025. 1

[15] Kangye Ji, Yuan Meng, Hanyun Cui, Ye Li, Shengjia Hua, Lei Chen, and Zhi Wang. Block-wise adaptive caching for accelerating diffusion policy. *ArXiv*, abs/2506.13456, 2025. 2, 3, 5, 6, 7

[16] Sehoon Kim, Karttikeya Mangalam, Suhong Moon, Jitendra Malik, Michael W Mahoney, Amir Gholami, and Kurt Keutzer. Speculative decoding with big little decoder. *Advances in Neural Information Processing Systems*, 36:39236–39256, 2023. 3

[17] Yaniv Leviathan, Matan Kalman, and Yossi Matias. Fast inference from transformers via speculative decoding. In *International Conference on Machine Learning*, 2022.

[18] Yaniv Leviathan, Matan Kalman, and Yossi Matias. Fast inference from transformers via speculative decoding. In *International Conference on Machine Learning*, pages 19274–19286. PMLR, 2023. 3

[19] Xiuyu Li, Yijiang Liu, Long Lian, Huanrui Yang, Zhen Dong, Daniel Kang, Shanghang Zhang, and Kurt Keutzer. Q-diffusion: Quantizing diffusion models. In *Proceedings of the IEEE/CVF International Conference on Computer Vision*, pages 17535–17545, 2023. 2, 3

[20] Ye Li, ZhongXin Liu, Ge Lan, Malika Sader, and ZengQiang Chen. A ddpg-based solution for optimal consensus of continuous-time linear multi-agent systems. *Science China Technological Sciences*, 66(8):2441–2453, 2023. 3

[21] Yuhui Li, Fangyun Wei, Chao Zhang, and Hongyang Zhang. Eagle: Speculative sampling requires rethinking feature uncertainty. *arXiv preprint arXiv:2401.15077*, 2024. 2, 3

[22] Yuhui Li, Fangyun Wei, Chao Zhang, and Hongyang Zhang. Eagle-2: Faster inference of language models with dynamic draft trees. *arXiv preprint arXiv:2406.16858*, 2024. 2, 3

[23] Ye Li, Yuan Meng, Zewen Sun, Kangye Ji, Chen Tang, Jiajun Fan, Xinzhu Ma, Shutao Xia, Zhi Wang, and Wenwu Zhu. Sp-vla: A joint model scheduling and token pruning approach for vla model acceleration. *arXiv preprint arXiv:2506.12723*, 2025. 2, 3, 6

[24] Ye Li, Chen Tang, Yuan Meng, Jiajun Fan, Zenghao Chai, Xinzhu Ma, Zhi Wang, and Wenwu Zhu. Prance: Joint token-optimization and structural channel-pruning for adaptive vit inference. *IEEE Transactions on Pattern Analysis and Machine Intelligence*, pages 1–17, 2025. 3

[25] Yuhui Li, Fangyun Wei, Chao Zhang, and Hongyang Zhang. Eagle-3: Scaling up inference acceleration of large language models via training-time test. *arXiv preprint arXiv:2503.01840*, 2025. 2, 3

[26] Feng Liu, Shiwei Zhang, Xiaofeng Wang, Yujie Wei, Haonan Qiu, Yuzhong Zhao, Yingya Zhang, Qixiang Ye, and Fang Wan. Timestep embedding tells: It's time to cache for video diffusion model. In *Proceedings of the Computer Vision and Pattern Recognition Conference*, pages 7353–7363, 2025. 3

[27] Jiacheng Liu, Chang Zou, Yuanhuiyi Lyu, Fei Ren, Shaobo Wang, Kaixin Li, and Linfeng Zhang. Speca: Accelerating diffusion transformers with speculative feature caching. In *Proceedings of the 33rd ACM International Conference on Multimedia*, pages 10024–10033, 2025. 3, 5, 6, 7

[28] Songming Liu, Lingxuan Wu, Bangguo Li, Hengkai Tan, Huayu Chen, Zhengyi Wang, Ke Xu, Hang Su, and Jun Zhu. Rdt-1b: a diffusion foundation model for bimanual manipulation. *arXiv preprint arXiv:2410.07864*, 2024. 1

[29] Yijun Liu, Yuwei Liu, Yuan Meng, Jieheng Zhang, Yuwei Zhou, Ye Li, Jiacheng Jiang, Kangye Ji, Shijia Ge, Zhi Wang, et al. Spatial policy: Guiding visuomotor robotic manipulation with spatial-aware modeling and reasoning. *arXiv preprint arXiv:2508.15874*, 2025. 1

[30] Zhongxin Liu, Ye Li, Ge Lan, and Zengqiang Chen. A novel data-driven model-free synchronization protocol for discrete-time multi-agent systems via td3 based algorithm. *Knowledge-Based Systems*, 287:111430, 2024. 3

[31] Ruben Martinez-Cantin, Nando de Freitas, A. Doucet, and José A. Castellanos. Active policy learning for robot planning and exploration under uncertainty. In *Robotics: Science and Systems*, 2007. 2

[32] Xiaohuan Pei, Yuxing Chen, Siyu Xu, Yunke Wang, Yuheng Shi, and Chang Xu. Action-aware dynamic pruning for efficient vision-language-action manipulation. *arXiv preprint arXiv:2509.22093*, 2025. 3

[33] Aditya Prasad, Kevin Lin, Jimmy Wu, Linqi Zhou, and Jeannette Bohg. Consistency policy: Accelerated visuomotor policies via consistency distillation. *ArXiv*, abs/2405.07503, 2024. 3

[34] John Schulman, Filip Wolski, Prafulla Dhariwal, Alec Radford, and Oleg Klimov. Proximal policy optimization algorithms. *arXiv preprint arXiv:1707.06347*, 2017. 7

[35] Yuzhang Shang, Zhihang Yuan, Bin Xie, Bingzhe Wu, and Yan Yan. Post-training quantization on diffusion models. In *Proceedings of the IEEE/CVF conference on computer vision and pattern recognition*, pages 1972–1981, 2023. 3

[36] Yuda Song, Zehao Sun, and Xuanwu Yin. Sdxs: Real-time one-step latent diffusion models with image conditions. *arXiv preprint arXiv:2403.16627*, 2024. 3

[37] Octo Model Team, Dibya Ghosh, Homer Walke, Karl Pertsch, Kevin Black, Oier Mees, Sudeep Dasari, Joey Hejna, Tobias Kreiman, Charles Xu, et al. Octo: An open-source generalist robot policy. *arXiv preprint arXiv:2405.12213*, 2024. 1

[38] Ben Wan, Tianyi Zheng, Zhaoyu Chen, Yuxiao Wang, and Jia Wang. Pruning for sparse diffusion models based on gradient flow. In *ICASSP 2025-2025 IEEE International Conference on Acoustics, Speech and Signal Processing (ICASSP)*, pages 1–5. IEEE, 2025. 2

[39] Zhendong Wang, Zhaoshuo Li, Ajay Mandlekar, Zhenjia Xu, Jiaoqiao Fan, Yashraj S. Narang, Linxi Fan, Yuke Zhu, Yogesh Balaji, Mingyuan Zhou, Ming-Yu Liu, and Yuan Zeng. One-step diffusion policy: Fast visuomotor policies via diffusion distillation. *ArXiv*, abs/2410.21257, 2024. 3

[40] Yantai Yang, Yuhao Wang, Zichen Wen, Zhongwei Luo, Chang Zou, Zhipeng Zhang, Chuan Wen, and Linfeng Zhang. Efficientvla: Training-free acceleration and compression for vision-language-action models. *ArXiv*, abs/2506.10100, 2025. 3

[41] Yantai Yang, Yuhao Wang, Zichen Wen, Luo Zhongwei, Chang Zou, Zhipeng Zhang, Chuan Wen, and Linfeng Zhang. Efficientvla: Training-free acceleration and compression for vision-language-action models. *arXiv preprint arXiv:2506.10100*, 2025. 2

[42] Jiaoqiao Ye, Zhen Wang, and Linnan Jiang. Pqd: Post-training quantization for efficient diffusion models. In *Proceedings of the Winter Conference on Applications of Computer Vision*, pages 150–156, 2025. 3

[43] Tianwei Yin, Michaël Gharbi, Richard Zhang, Eli Shechtman, Fredo Durand, William T Freeman, and Taesung Park. One-step diffusion with distribution matching distillation. In *Proceedings of the IEEE/CVF conference on computer vision and pattern recognition*, pages 6613–6623, 2024. 3

[44] Zhaoshu Yu, Bo Wang, Pengpeng Zeng, Haonan Zhang, Ji Zhang, Lianli Gao, Jingkuan Song, Nicu Sebe, and Heng Tao Shen. A survey on efficient vision-language-action models. *arXiv preprint arXiv:2510.24795*, 2025. 3

[45] Qian Zeng, Chenggong Hu, Mingli Song, and Jie Song. Diffusion model quantization: A review. *arXiv preprint arXiv:2505.05215*, 2025. 3

[46] Dingkun Zhang, Sijia Li, Chen Chen, Qingsong Xie, and Haonan Lu. Laptop-diff: Layer pruning and normalized distillation for compressing diffusion models. *arXiv preprint arXiv:2404.11098*, 2024. 2

[47] Shikang Zheng, Guantao Chen, Qinming Zhou, Yuqi Lin, Lixuan He, Chang Zou, Peiliang Cai, Jiacheng Liu, and Linfeng Zhang. Let features decide their own solvers: Hybrid feature caching for diffusion transformers. *arXiv preprint arXiv:2510.04188*, 2025. 3

[48] Hongyi Zhou, Denis Blessing, Ge Li, Onur Celik, Xiaogang Jia, Gerhard Neumann, and Rudolf Lioutikov. Variational distillation of diffusion policies into mixture of experts. *ArXiv*, abs/2406.12538, 2024. 3

[49] Yuanzhi Zhu, Eleftherios Tsonis, Lucas Degeorge, and Vicky Kalogeiton. One-step diffusion models with bregman density ratio matching. *arXiv preprint arXiv:2510.16983*, 2025. 3

[50] Chang Zou, Xuyang Liu, Ting Liu, Siteng Huang, and Linfeng Zhang. Accelerating diffusion transformers with token-wise feature caching. *arXiv preprint arXiv:2410.05317*, 2024. 3

[51] Chang Zou, Evelyn Zhang, Runlin Guo, Haohang Xu, Conghui He, Xuming Hu, and Linfeng Zhang. Accelerating diffusion transformers with dual feature caching. *arXiv preprint arXiv:2412.18911*, 2024. 3

TS-DP: Reinforcement Speculative Decoding For Temporal Adaptive Diffusion Policy Acceleration

Supplementary Material

6. A. Detailed Benchmark Results

Tables 1, 2, and 3 present comprehensive benchmark results across all evaluated datasets, reporting four critical metrics: Number of Function Evaluations (NFE), inference speedup factor, draft count, and draft acceptance rate. Our results demonstrate consistent acceleration across all benchmarks while maintaining high draft acceptance rates. On the Proficient Human dataset, TS-DP achieves uniform acceleration with NFE reduced to 24.0 of the baseline on average, yielding a speedup of 4.17 \times while maintaining a draft acceptance rate of 85.2%. On the Mixed Human dataset, the framework maintains robust performance with NFE at 26.28 of baseline on average and a speedup of 3.83 \times , while achieving a draft acceptance rate of 87.1%.

For multi-stage tasks, TS-DP exhibits remarkable consistency across all subtasks. The framework achieves an average speedup of 3.77 \times with NFE at 27.2 of baseline while maintaining high draft acceptance rates. The draft count remains consistently high between 88.6 and 94.1 across all scenarios, confirming the effectiveness of our temporal complexity aware scheduling. These comprehensive metrics validate that TS-DP achieves both extreme computational efficiency and high draft fidelity across diverse robotic manipulation scenarios, with consistent performance across different task categories demonstrating robustness to varying embodiment complexities and environmental dynamics.

7. B. Visualization Analysis

Figure 1 provides detailed visualizations of draft acceptance rates and draft counts across the six primary tasks from the Proficient Human dataset. The comparison between TS-DP (red) and the fixed-parameter baseline (green) reveals a clear pattern of adaptive behavior: TS-DP maintains consistently higher acceptance rates while dynamically adjusting draft counts according to task phase complexity. During stable execution phases as observed in Transport and Square tasks, our framework increases draft count to maximize parallelism, whereas during critical manipulation phases characteristic of Tool and Can tasks, it intelligently reduces draft count while maintaining high acceptance rates.

This contrast highlights the fundamental limitation of fixed-parameter approaches: they cannot adapt to the varying temporal complexity inherent in embodied tasks such as Lift, Can, and Push-T. TS-DP’s dynamic adjustment of speculative parameters enables optimal balance between acceleration and accuracy throughout the execution process.

Algorithm 1: TS-DP: Temporal-Speculative Diffusion Decoding.

```
Input:  $\varphi$ , target model  $\mathcal{M}_T$ , drafter  $\mathcal{M}_D$ ,  $L, \tau, \lambda$ 
Output:  $S$ 
Initialize cache  $\mathcal{C}$ ;  $z, f_0 \leftarrow \mathcal{M}_T(\varphi)$ ;  $S = \emptyset, v_{\text{last}} = \text{True}$ 
for  $t = 0$  to  $L - 1$  do
     $C_t \leftarrow \mathcal{M}_D(f_t, z)$ 
    skip  $\leftarrow \text{Decision}(C_t, t, v_{\text{last}}, \tau)$ 
    if not skip then
         $(\ell_t, h_t) \leftarrow \mathcal{M}_T(z \oplus C_t)$ 
        // Draft acceptance
         $p_i = \min(1, \exp(-\frac{1}{2}\|d_i\|^2 - \langle d_i, \xi_i \rangle))$ 
         $d_i = \frac{\hat{\mu}_i - \mu_i}{\sigma_i}$ 
         $x \leftarrow \text{Verify}(p_i, C_t, \lambda)$ 
         $\mathcal{C} \leftarrow \text{UpdateCache}(h_t)$ 
         $f_t \leftarrow \text{Retrieve}(\mathcal{C}, x)$ 
         $v_{\text{last}} \leftarrow \text{False}$ 
         $S \leftarrow S \oplus x$ 
    else
         $x^\circ \leftarrow \text{UniformSample}(C_t)$ 
        // Reflection-maximal coupling
         $x = \mu + (I - 2ee^\top)(\hat{x} - \hat{\mu}), \quad e = \frac{\hat{\mu} - \mu}{\|\hat{\mu} - \mu\|}$ 
         $f_t \leftarrow \text{RetrieveStale}(\mathcal{C}, x^\circ)$ 
         $v_{\text{last}} \leftarrow \text{True}$ 
         $S \leftarrow S \oplus x^\circ$ 
    end
return  $S$ 
```

The consistent temporal adaptation patterns directly correlate with the high draft acceptance rates reported in benchmark tables, confirming that our method effectively addresses the dynamic complexity of embodied tasks through intelligent scheduling rather than relying on static configuration.

8. C. Algorithm Flow

Algorithm 1 summarizes the TS-DP decoding process. The drafter generates speculative denoising steps, while the target model verifies them through a lightweight acceptance test. Accepted steps allow the algorithm to advance multiple timesteps efficiently, whereas rejected ones are refined via reflection coupling to preserve the exact diffusion dynamics.

Table 1. **Benchmark on Proficient Human (PH) demonstration data.** Reported metrics per task: NFE, Speed, Draft count, and Acceptance rate.

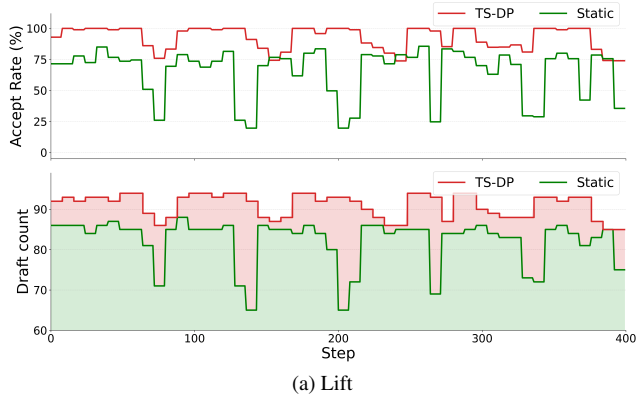
Metric	Task						AVG
	Lift	Can	Square	Transport	Tool	Push-T	
NFE	24.4 / 24.4	23.8 / 24.7	24.3 / 24.3	23.3 / 23.4	24.3 / 24.2	23.9 / 23.9	24.0 / 24.1
Speed (×)	4.1 / 4.1	4.2 / 4.0	4.1 / 4.1	4.3 / 4.3	4.1 / 4.1	4.2 / 4.2	4.17 / 4.13
Draft count	93.7 / 93.7	93.9 / 93.5	93.8 / 93.7	94.1 / 94.1	93.7 / 93.8	94.0 / 94.0	93.87 / 93.80
Acceptance rate (%)	84.5 / 84.5	85.3 / 85.3	85.2 / 84.6	86.7 / 86.7	84.8 / 84.9	84.7 / 84.7	85.2 / 85.1

Table 2. **Benchmark on Proficient Human (MH) demonstration data.** Reported metrics per task: NFE, Speed, Draft count, and Acceptance rate.

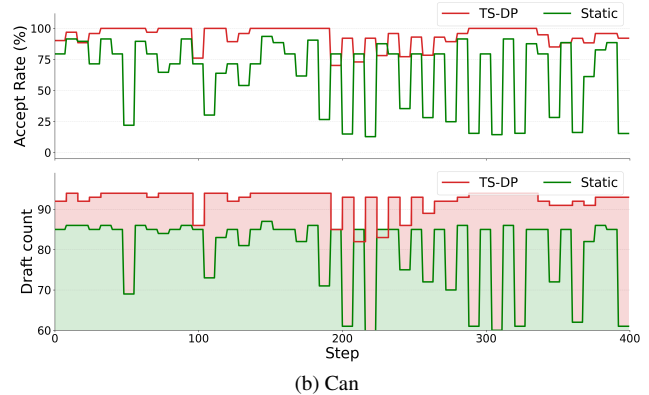
Metric	Task				AVG
	Lift	Can	Square	Transport	
NFE	28.1 / 28.1	25.7 / 26.1	26.6 / 26.7	24.7 / 24.7	26.28 / 26.40
Speed (×)	3.6 / 3.6	3.9 / 3.8	3.8 / 3.8	4.0 / 4.0	3.83 / 3.80
Draft count	91.7 / 91.7	92.7 / 92.5	92.35 / 92.31	93.1 / 93.0	92.46 / 92.38
Acceptance rate (%)	84.4 / 84.0	88.0 / 87.8	86.3 / 85.8	89.7 / 89.4	87.1 / 86.7

Table 3. **Benchmark on multi-stage task (Kitchen & BP).** Reported metrics per task: NFE, Speed, Draft count, and Acceptance rate.

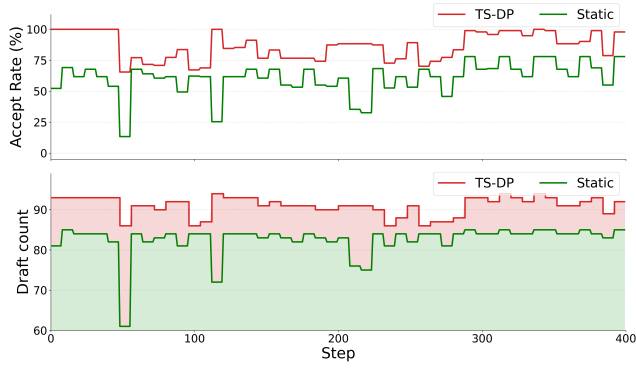
Metric	Task						AVG
	BP _{p1}	BP _{p2}	Kit _{p1}	Kit _{p2}	Kit _{p3}	Kit _{p4}	
NFE	34.0 / 34.0	34.0 / 34.0	23.8 / 23.9	23.8 / 23.9	23.8 / 23.9	23.8 / 23.9	27.2 / 27.3
Speed (×)	2.9 / 2.9	2.9 / 2.9	4.2 / 4.2	4.2 / 4.2	4.2 / 4.2	4.2 / 4.2	3.77 / 3.77
Draft count	88.7 / 88.6	88.7 / 88.6	93.3 / 93.3	93.3 / 93.3	93.3 / 93.3	93.3 / 93.3	91.8 / 91.8
Acceptance rate (%)	82.7 / 82.6	82.7 / 82.6	93.3 / 93.3	93.3 / 93.3	93.3 / 93.3	93.3 / 93.3	89.8 / 89.8



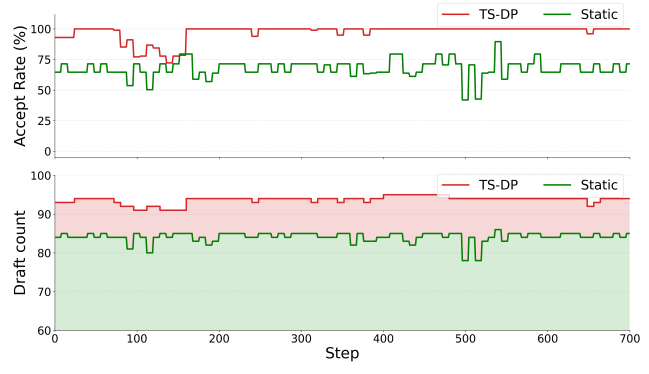
(a) Lift



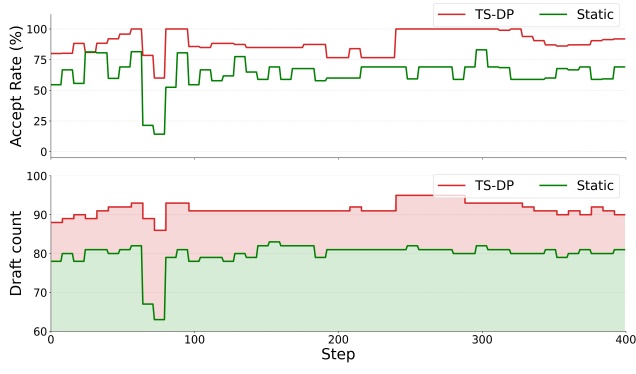
(b) Can



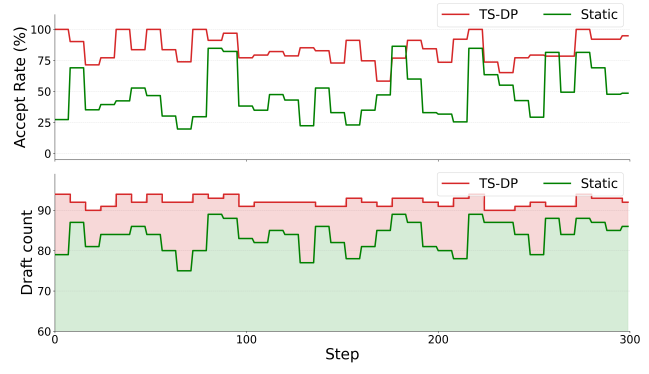
(c) Square



(d) Transport



(e) Tool



(f) Push-T

Figure 1. Effect of TS-DP on Acceptance Rate and Draft Count. (Top) Acceptance Rate; (Bottom) Draft Count.